Introduction of Compressive Residual Stresses in Ti-6Al-4V Simulated Airfoils via Laser Shock Processing

M.J. Shepard, P.R. Smith, and M.S. Amer

(Submitted 21 May 2001)

Ti-6Al-4V (Ti-64) simulated airfoils were laser shock processed with two laser power densities (4 and 9 GW/^{2}) for each of three pulse repetition treatments (1, 3, and 5 shocks/spot). The microstructural effects of laser shock processing (LSP) on the Ti-64 were studied *via* scanning electron microscopy (SEM). Ultrasonic nondestructive inspection (NDI) was conducted to ensure that the LSP treatments resulted in no internal damage to the simulated airfoils. In-depth residual stress and cold work measurements were made using x-ray diffraction.

No substantial changes due to LSP were found in the microstructure, and no internal damage was detected during NDI or metallographic sectioning. It was found that the in-depth residual stress and cold work states induced by LSP were a function of laser power density and pulse repetition. It was possible to induce compressive residual stresses in the direction most critical for the prevention of fatigue-crack growth throughout the thickness of the simulated airfoil leading edge.

Keywords component surface treatment, laser shock processing, LSP, residual stress, Ti-6Al-4V

1. Introduction and Background

The introduction of compressive residual stresses in the surface layers of components that are to be cyclically loaded can result in an increase in fatigue life. This is derived largely from the fact that, in order for a fatigue crack to propagate, the region at the crack tip must be in a state of tension during some point in the loading cycle. When a residual state of compressive stress has been superimposed over the stress state resulting from service loading, it is possible that most or all of the load spectrum will remain in the compression region. For applications, such as gas turbine-engine blades, such fatigue enhancements are critical, since at the rotational speeds at which gas turbine engines operate (thousands of rpm), cracks initiated by foreign object damage (FOD) can potentially propagate and result in premature failure.

Turbine engine manufacturers have long sought the introduction of beneficial states of residual stress in their engine components through a variety of means. The most common of these is shot peening.[1] Shot peening is inexpensive, and the improvements in fatigue life from this process are well documented. Unfortunately, though, there are some disadvantages to this process. First, the depth to which the workpiece can be imparted with a compressive residual stress state *via* shot peening is quite limited, usually on the order of a few tenths of a millimeter. Furthermore, this process is usually associated with high levels of surface cold work.[2]

M.J. Shepard and **P.R. Smith**, Air Force Research Laboratory, Materials and Manufacturing Directorate, Wright-Patterson AFB, OH 45433-7817; and **M.S. Amer**, Department of Mechanical and Materials Engineering, Wright State University, Dayton, OH, 45435-0001. Contact e-mail: michael.shepard@afrl.af.mil.

These two limitations are less than ideal in a high-performance turbine engine environment. The shallow depth to which shot peening imparts the compressive residual stress limits the process's ability to effectively combat large FOD, which may cause initial damage (cracking or material loss) that is larger than the depth of the compressive residual-stress layer. Additionally, high cold work, in conjunction with engine service temperatures, leads to a large driving force for relief of the induced compressive residual stresses.[2] Finally, the highly strain-hardened surface layers can make the compressive residual stress susceptible to mechanical relief or inversion to residual tensile stress during momentary overload.[3]

1.1 Laser Shock Peening

Laser shock peening is one alternative method for introducing compressive residual stresses into the surfaces of components. In this process, a laser beam is used to vaporize a thin opaque coating (often flat black paint) applied to the surface of the component over the region to be treated. The vaporization of the paint produces a rapidly expanding plasma that is confined against the surface of the component by a constraining layer (usually water) that is transparent to the laser. The pressure at the surface of the component increases rapidly, thereby causing a compressive shock wave to travel into the material. If this shock wave is of sufficient magnitude, the peak pressures will exceed the Hugonoit elastic limit (dynamic yield stress under shock conditions) of the material and the shocked region will undergo plastic deformation. The strain rates can be as high as 10^6/s.[4] After the shock wave dissipates, the region is left in a state of compressive stress due to the constraint from undeformed material outside of the treated region. As a result, offsetting tensile states of stress are found outside of the processed regions, typically in areas that are deemed to be less susceptible to fatigue or FOD damage. The laser shock peening process is shown schematically in Fig. 1. Further details on the laser shock peening process can be found elsewhere.[5,6]

Information regarding the laser shock peening process in

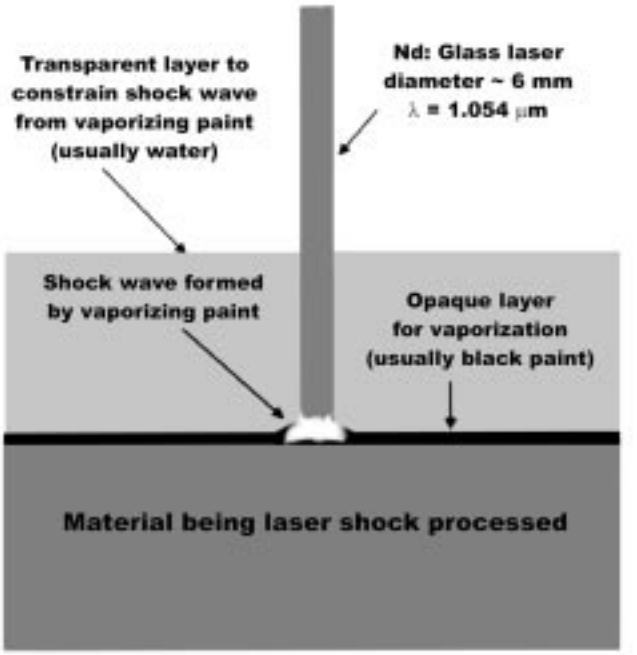

Fig. 1 Schematic of laser shock peening process

the public domain, while adequate in some aspects (*e.g.*, effects of transparent and opaque overlays), is lacking in others. One of these underdeveloped areas is the effect of laser power density and pulse repetition on the laser shock peening of complex workpieces, such as turbine engine blades. Due to the uncertainties associated with the geometrically induced shock-wave interactions and yielding criterion at extremely high strain rates,[4] the current state-of-the-art numerical modeling has, to date, proven unsuccessful at modeling the induced residual stresses in complex workpieces. Hence, it becomes necessary to empirically explore the LSP-induced residual stress and cold work states under such complex treatment conditions and part geometry. In this paper, we report the state of residual stress and cold work resulting from dual-sided simultaneous shocking of a simulated airfoil geometry. The effect of laser power density and pulse repetition on residual stress and cold work is also reported and discussed.

2. Experimental Methods

2.1 Material

The Ti-64 material selected for the subject study was taken from forgings that have a microstructure representative of that used for turbine-engine fan blades. The forging stock was taken from double vacuum-arc-remelted, Ti-64 63.5 mm diameter bar stock produced in accordance with ASM 4928 in a mill annealed condition (705 °C/2 h/AC). Forging multiples 406.4 mm long were preheated to 938 °C (±11 °C) for a minimum of 30 min prior to forging. The forgings were then solution treated (932 °C (±14 °C) for 75 min/fan air cool) to maximize chemical and microstructural uniformity throughout the forging. The forgings were then cleaned using caustic acid baths and grit blasting to remove oxides and any alpha case that may have formed. The

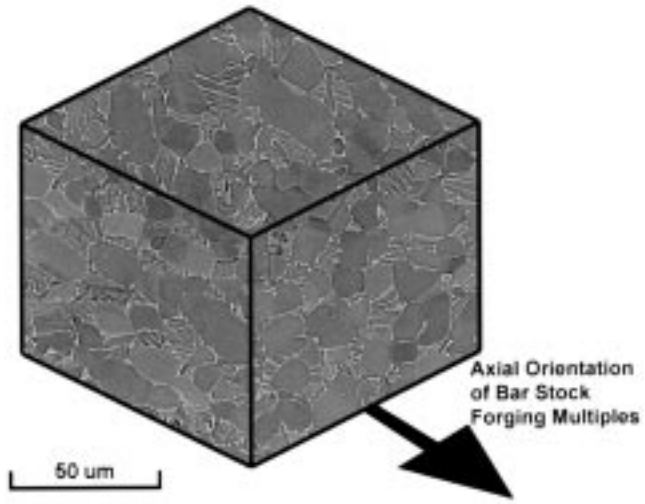

Fig. 2 Ti-6Al-4V microstructure as used in the present study

Table 1 Chemical composition of study material as compared to AMS 4928

Element	AMS 4928 (wt %)	Study material (wt.%)
Al	5.50 to 6.75	6.24
V	3.50 to 4.50	4.2
Fe	0.30 max	0.19
O	0.20 max	0.172
N	0.050 max	0.009
C	…	0.0191
H	…	43.67 ppm
Ni	…	0.032
Cu	…	<0.05
Mo	…	<0.02
Nb	…	<0.05
Zr	…	<0.05
Ti	Bal.	Bal.

forgings were vacuum annealed (705 °C (±14 °C) for 2 h/argon fan cool) to stabilize the microstructure and normalize hydrogen content.

The microstructure of the forgings consists of ~60% primary alpha, with the remaining 40% consisting of a transformed beta structure (Fig. 2). This latter microstructural constituent is further composed of lenticular alpha (dark) and intergranular beta (light) phases. The microstructure is relatively equiax, with only slight elongation along the longitudinal axis of the forging, as shown in Fig. 2. This axis corresponds with the axial orientation of the bar-stock forging multiples.

Longitudinal tensile properties were assessed at a strain rate $= 5 \times 10^{-4\ -1}$, yield strength = 930 MPa, ultimate tensile strength = 978 MPa, and modulus = 118 GPa. Tensile properties in the transverse direction were also tested and were very similar in magnitude.[7]

A chemical analysis was conducted to validate the chemistry of the material, in particular, to ensure that the interstitial content was not unduly high. The results of this analysis, found in Table 1, show that the major alloying elements are well within manufacturers specifications. Additionally, interstitial content is not high.

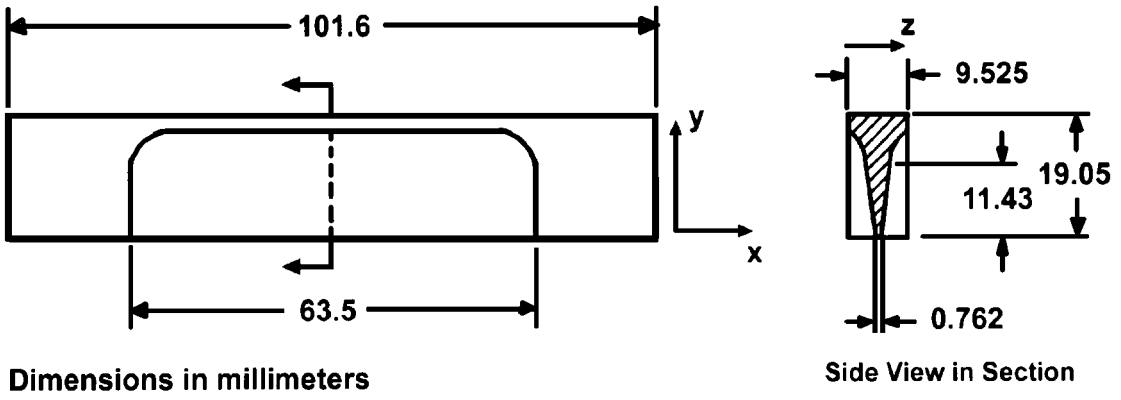

Fig. 3 Schematic of 3-point bend simulated airfoil specimen

2.2 Specimen Geometry Selection

The specimen geometry selected for this study was designed for a previous LSP investigation.[8] Simulated airfoil specimens were milled to shape and then low-stress ground to final dimensions (Fig. 3) from the aforementioned Ti-64 plates. The design of these specimens was intended to approximate a leading edge geometry of an airfoil with a thickness of 0.75 mm. The thickness of the specimen is tapered to provide a thin section along one edge, which enables through-thickness compressive residual stresses to be generated in this region *via* LSP. In the thicker internal regions and outside the area of LSP treatment, tensile residual stresses develop to counterbalance the compressive stresses in the LSP zone.

This simulated airfoil specimen is representative of a generic compressor blade and allows for an empirical evaluation of the residual stresses and cold work generated by varying laser power density and pulse repetition. This is critical since the residual stresses and cold work generated by LSP are very geometry dependent and difficult to model.[4]

Previous studies suggested that the superposition of residual stresses due to laser shock peening upon those induced by machining makes the effects of laser intensity difficult to discern.[9] This is due to the fact that the stresses associated with machining can be of surprisingly high magnitude and induce considerable cold work. As such, all specimens were stress relief annealed at 704 °C/1 h in a vacuum ($\sim 10^{-6}$ torr) followed by a furnace cool to reduce or eliminate residual stresses and cold work due to machining. Additional details regarding the development of this specimen geometry and the rationale for its use in conjunction with LSP studies can be found elsewhere.[8]

2.3 Laser Power and Pulse Repetition

All LSP was carried out at LSP Technologies (Dublin, OH). In this work, two LSP power densities were selected, 4 and 9 GW/cm^2, representing a low laser power density and a high laser power density, respectively. Shock waves generated by laser pulses below 4 GW/cm^2 are unlikely to be intense enough to generate plastic deformation sufficient to produce a compressive residual stress of any substantial magnitude. Previous work has demonstrated that 9 GW/cm^2 was a reasonable upper limit in thin sections due to gross plastic deformation[10] and the onset of dielectric breakdown of the transparent overlay.[6]

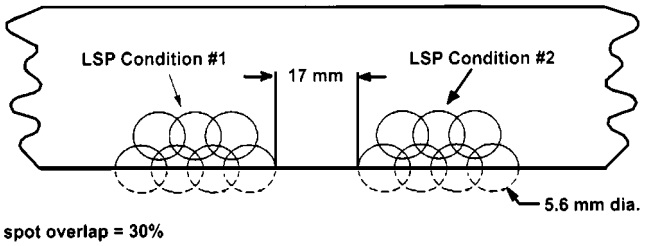

Fig. 4 The LSP spot patterns used for x-ray diffraction and microstructural analysis

Previous work has shown that repeated shocking can both increase the magnitude of the residual stress field and drive the peak residual stresses deeper into the material, much as in the case of traditional shot peening.[6,11] As such, three pulse repetition schemes were studied: 1, 3, and 5 shocks/spot. Laser pulse duration was kept constant at 20 ns. The laser used for all LSP was an Nd:phosphate glass laser with a wavelength $\lambda = 1.054$ μm.

The transparent overlay and opaque coating for this investigation were water and flat black paint, respectively. Water was selected primarily because of its ease of use. Black paint was selected not only for its ease of use, but also because its effectiveness is equal to or greater than other explored alternatives used for generating high peak shock-wave pressures at a given laser power density.[12]

The LSP spot pattern used in this study consisted of two LSP patches arranged as shown in Fig. 4. One of the patches was used for the collection of x-ray diffraction data, while the other patch was sectioned for microstructural evaluation *via* scanning electron microscopy (SEM). The LSP spots were overlapped ~30% in both the lateral (along the specimen length) and vertical (across the specimen height) directions. A finite element model was developed by Lambda Research (Cincinnati, OH) to ensure that the stress fields from the two LSP patches found on the airfoils would not overlap.

2.4 Residual Stress and Cold Work Measurements

Residual stress and percent cold work measurements were made at Lambda Research. All measurements were made near

the center of the LSP-treated area using x-ray diffraction in accordance with recommendation SAE J784a and ASTM specifications E915 and E1426. Material was removed electrolytically for subsurface measurement in order to minimize alterations in the stress distributions that would be caused by machining or grinding. Residual stress results were corrected for penetration of the radiation into the stress gradient and for stress relaxation due to the material removal using a finite element model of the specimen geometry developed by Lambda Research. The percent cold work was estimated by correlating the diffraction peak width to true plastic strain, as described by Prevéy.[13,14] Assuming symmetry in the compressive residual-stress state due to the simultaneous application of LSP to both sides of the specimen, residual stress and percent cold work measurements were made through half the nominal thickness. All reported residual stresses are oriented in the *x* direction, as indicated in Fig. 3.

2.5 SEM Evaluation

Specimen preparation for microstructural evaluation was carried out using standard metallographic techniques. Etching was accomplished with Kroll's Reagent (1 HF, 9 HCL, and 90 H_2O). Two orientations in the laser shock processed region were examined for each of the six LSP treatments, an unprocessed airfoil: the "face" of the blade in the LSP zone and a transverse cross section of the blade. Microstructural evaluation was conducted using a Leica 360 FE scanning electron microscope in backscatter electron imaging mode with a maximum resolution of 2 nm.

Digital image analysis for phase content was accomplished using NIH Image 1.62 for Power Macintosh computers, available free of charge from the National Institutes of Health (Bethesda, Maryland). Density slicing techniques were used, wherein the histogram peak associated with the light phase (beta) was selected allowing the enumeration of the pixels composing the beta phase in the examined micrograph. This was then compared with the known total of pixels to yield the volume fraction of the beta phase. The volume fraction of the remaining phase (alpha) was found by subtraction.

2.6 Ultrasonic Nondestructive Inspection

Ultrasonic nondestructive inspection (NDI) was used to detect any internal damage (*i.e.*, cracking) due to LSP. All inspections were conducted using the NDI facilities of the Materials and Manufacturing Directorate at the Air Force Research Laboratory. All scans were collected with a 50 MHz, 12.7 mm, focal-length acoustic-microscope transducer. For each LSP condition, a C-scan image of the time-of-flight (TOF) data from the back-surface echo and any delaminations was collected. A C-scan image of the peak-to-peak amplitude of that echo was also collected. The resolution for this apparatus with simulated airfoil specimens is ~0.5 mm for midthickness flaws.

3. Experimental Results

3.1 Scanning Electron Microscopy

Microstructural characteristics of LSP treated and untreated regions were essentially indistinguishable except for minor

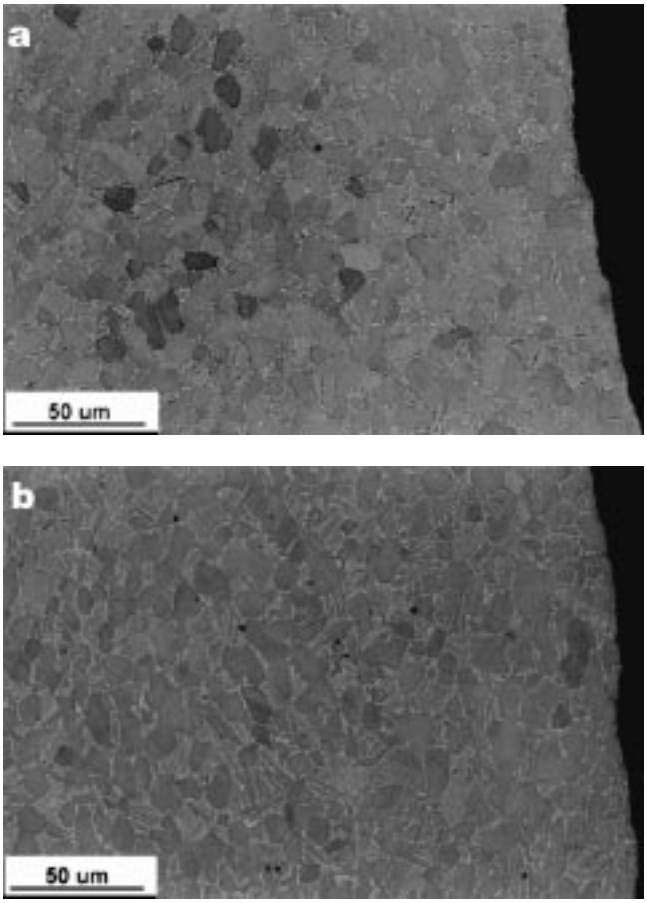

Fig. 5 Microstructure from a transverse cross section of the airfoil in the (**a**) baseline and (**b**) 9 GW/cm^2-5 shock/spot conditions

elongation of the grains in the transverse sections of the most intensely laser shock processed specimens (9 GW/cm^2-5 shocks). The elongation was quite modest and was in the direction perpendicular to shock-front propagation. Micrographs of this condition and the baseline condition are shown in Fig. 5. Micrographs of the baseline and the 9 GW/cm^2-5 shock condition taken from just beneath the surface of the face of the airfoil are shown in Fig. 6.

Other than the 9 GW/cm^2-5 shock condition, none of the other LSP treatments displayed differences in phase content or morphology from the baseline condition. In addition, no microcracking or other small-scale damage was detected.

3.2 Residual Stresses

Throughout this section, it should be noted that the residual stresses measured are those oriented in the *x* direction, as shown in Fig. 3. The depth dimension is the *z* direction, also as indicated in Fig. 3. As discussed in Section 2, the residual stress measurements stop at nominal midthickness and are corrected for material removal by assuming identical residual-stress distributions on each face of the airfoil specimen.

Baseline Residual Stress Condition. The in-depth residual-stress profiles for the baseline (non-laser shock processed) condition is shown in Fig. 7. It can be seen that the stress relief

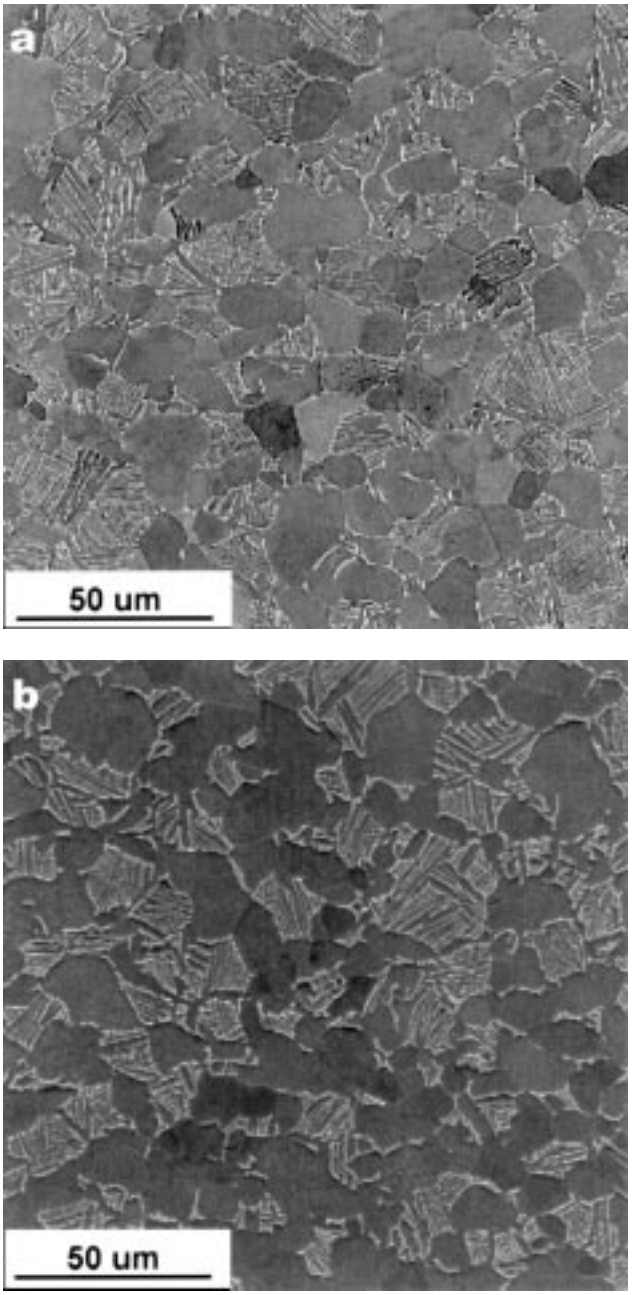

Fig. 6 Microstructure from a face orientation of the airfoil in the (**a**) baseline and (**b**) 9 GW/cm^2-5 shock/spot conditions

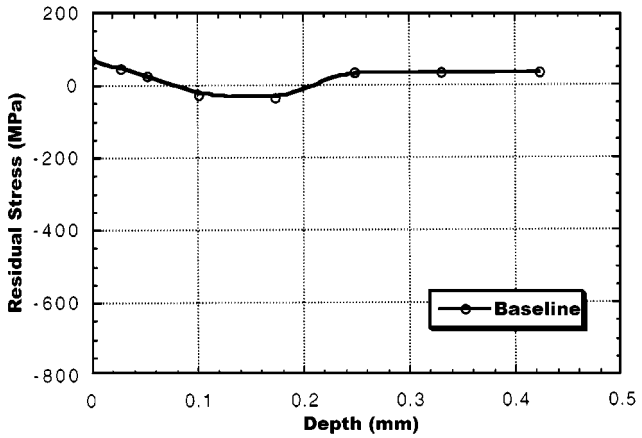

Fig. 7 Residual stress vs depth for baseline condition (pre-LSP)

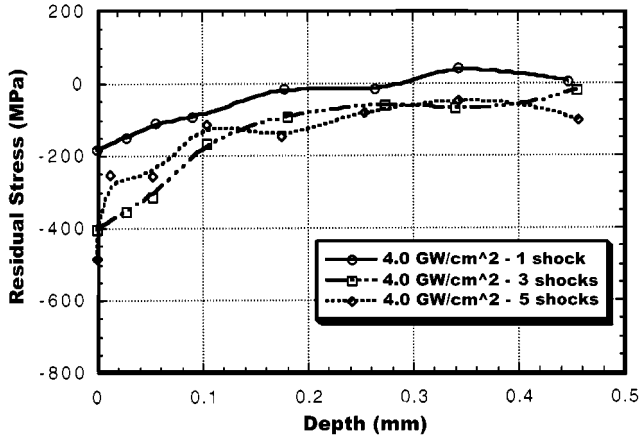

Fig. 8 Residual stress vs depth for 4 GW/cm^2 LSP trials

anneal has reduced the residual stress profile to a near zero state throughout the specimen thickness, thereby eliminating any effects of specimen machining.

Effects of Pulse Repetition on Residual Stresses. In Fig. 8, the residual stress results from the 4 GW/cm^2 trials are plotted. It can be seen that the magnitude of the compressive residual stresses increase with increasing pulse repetition. This effect is considerably more pronounced at the surface, while becoming considerably less pronounced beyond depths between 0.1 and 0.2 mm, where the residual stresses appear to reach a near steady-state level.

Immediately below the surface, though, the 3 and 5 shocks/spot repetition rates result in stress states that are very similar. In fact, at some depths, the 3 shock stresses were nominally more compressive than those found in the 5 shock stress field.

While both the 3 and 5 shock stress profiles are more compressive for all depths than the 1 shock profile, it seems that pulse repetition greater than 3 shocks offers no substantial residual-stress benefit, except, perhaps, at the very surface of the specimen.

Similar trends to those seen for the 4 GW/cm^2 trials can be observed in the stress profiles for the 9 GW/cm^2 trials depicted in Fig. 9. Again, the 3 and 5 shock/spot trials were very similar, this time there being no residual stress benefit for the 5 shock treatments, even at the surface.

Effects of Laser Intensity on Residual Stresses. Plotted in Fig. 10, 11, and 12 are the residual stress profiles associated with the 1, 3, and 5 shocks/spot trials, respectively. For each pulse repetition treatment, the 9 GW/cm^2 treatments produced more intense residual stresses, particularly at the surface, than the 4 GW/cm^2 treatments.

3.3. Cold Work

Baseline Cold Work Condition. Cold work measurements were made for the pre-LSP condition and for each of the six

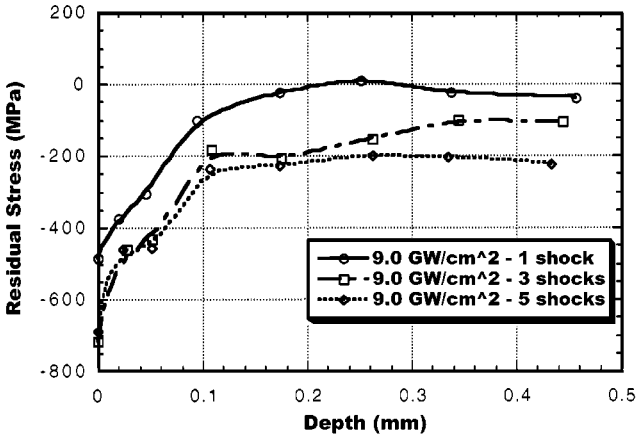

Fig. 9 Residual stress vs depth for 9 GW/cm^2 LSP trials

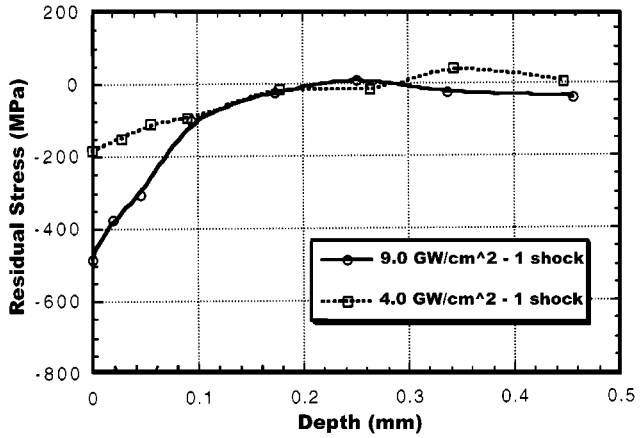

Fig. 10 Residual stress vs depth for 1 shock/spot trials

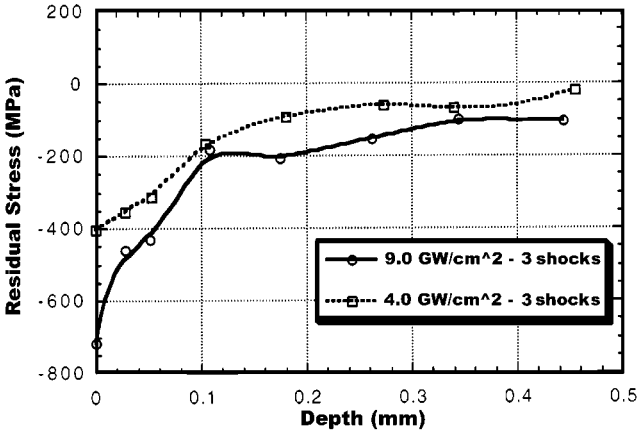

Fig. 11 Residual stress vs depth for 3 shock/spot trials

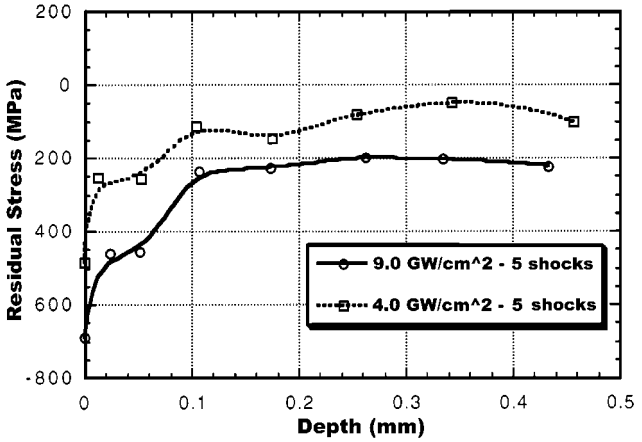

Fig. 12 Residual stress vs depth for 5 shock/spot trials

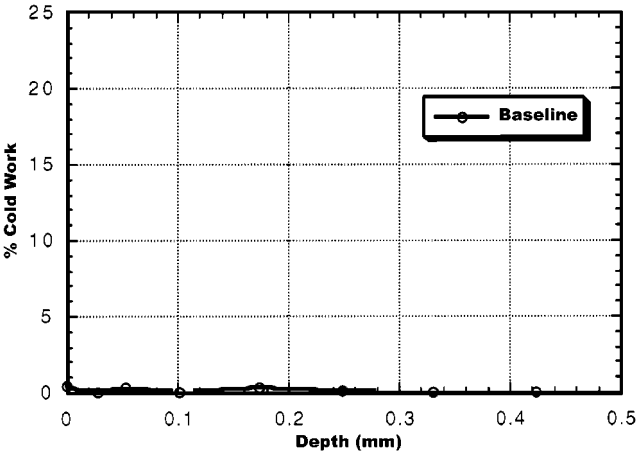

Fig. 13 In-depth baseline cold work condition (pre-LSP)

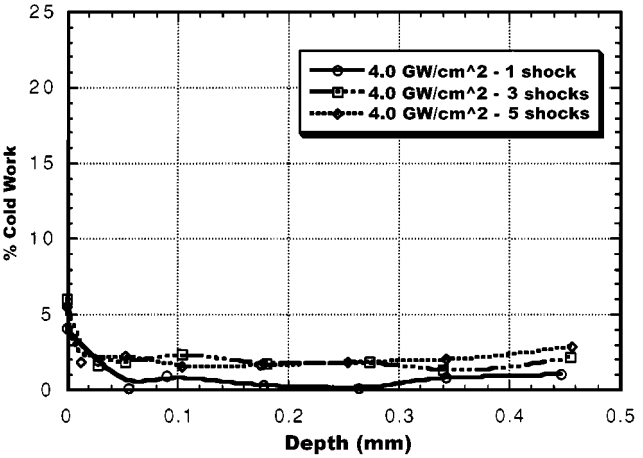

Fig. 14 Cold work vs depth for 4 GW/cm^2 conditions

sets of LSP conditions. Figure 13 depicts the in-depth cold work state of the un-LSP condition. The level of cold work was found to be zero or near zero through the thickness, after the stress relief anneal. This ensures that virtually all the cold work found in laser shock processed specimens would be due to the LSP and not to specimen machining.

Effects of Pulse Repetition on Cold Work. Figures 14 and

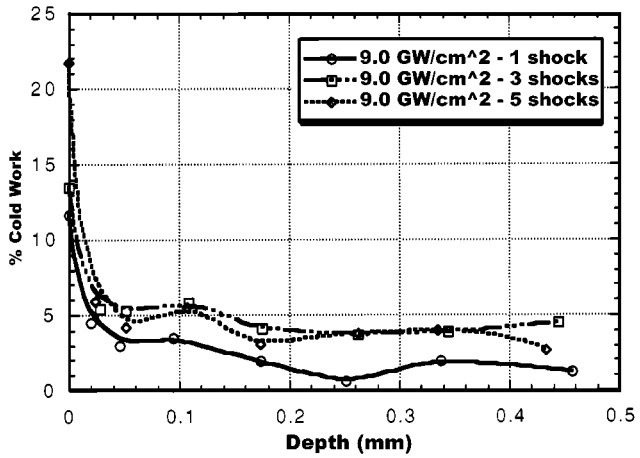

Fig. 15 Cold work vs depth for 9 GW/cm^2 conditions

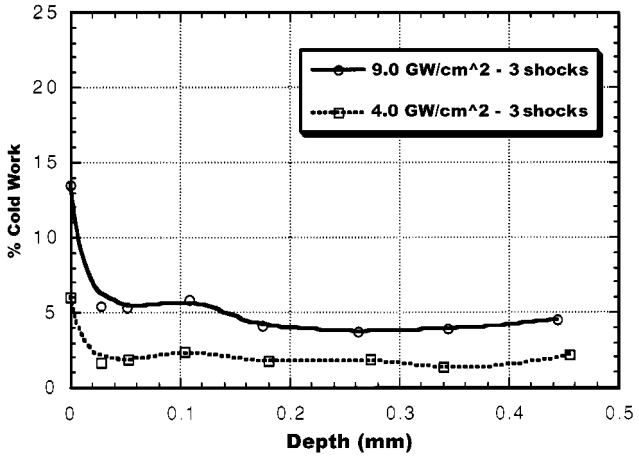

Fig. 17 Cold work vs depth for 3 shock/spot treatments

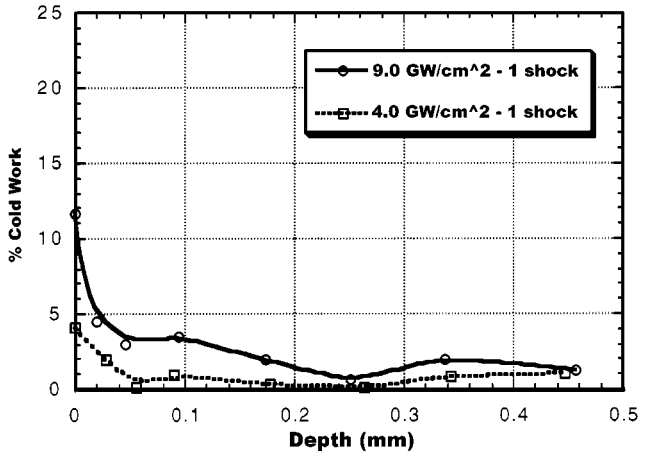

Fig. 16 Cold work vs depth for 1 shock/spot treatments

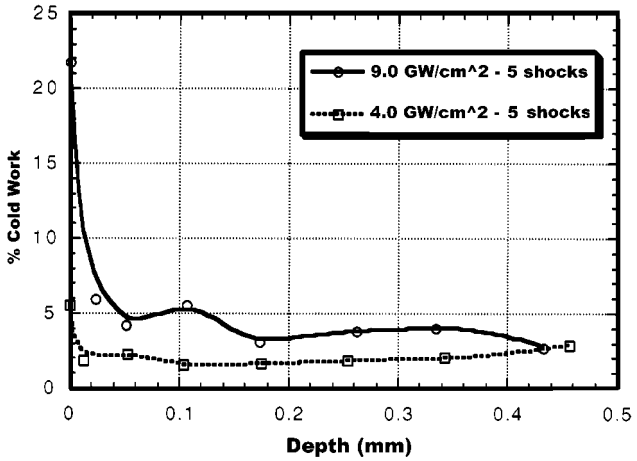

Fig. 18 Cold work vs depth for 5 shock/spot treatments

15 show the in-depth cold work states for the 4 GW/cm^2 and 9 GW/cm^2 treatments, respectively. For each laser intensity, increasing pulse repetition from 1 to 3 increased the level of cold work. The 5 shocks/spot repetition treatments produced cold work profiles that were generally similar to the 3 shocks/spot profiles (with the exception of the surface cold work in the 9 GW/ cm^2-3 and 5 shock treatments) at the same laser intensity, suggesting a similar saturation to that seen earlier in the residual stress data.

Effects of Laser Intensity on Cold Work. As can be seen in Fig. 16 to 18, for all pulse repetitions, the 9 GW/cm^2 treatment produces more cold work than the corresponding 4 GW/cm^2 conditions. Even the lightest 9 GW/cm^2 treatment (1 shock/spot) produced more cold work than the most intense 4 GW/cm^2 condition (5 shocks/spot) throughout the specimen thickness. This effect is most pronounced at the surface and gradually diminishes with increasing depth.

3.4 Ultrasonic Nondestructive Inspection

In the present study, the NDI results indicated no internal damage had occurred for any of the LSP parameters utilized, including the 5 shock/spot treatments. Additionally, extensive metallographic sectioning of the LSP zones corroborated the NDI results of no internal damage.

A peak-to-peak amplitude C-scan of the TOF echo from a water-immersion ultrasonic inspection for the most intense laser shock peening treatments, 9 GW/cm^2-5 shock/spot, is shown in Fig. 19. Although the imprints in the surface and a slight extrusion of the leading edge due to LSP can clearly be seen, there are no indications of internal delaminations.

4. Discussion

4.1 Distortion

Although no rigorous study of component distortion associated with LSP was made, a few comments are in order. Setting a limit for component distortion will be highly dependent on the application. If FOD-induced failures are a driving concern, some loss of aerodynamic efficiency, due to distortion, may be acceptable. Keeping this in mind, distortion sufficient to cause interference with other engine components is clearly unacceptable.

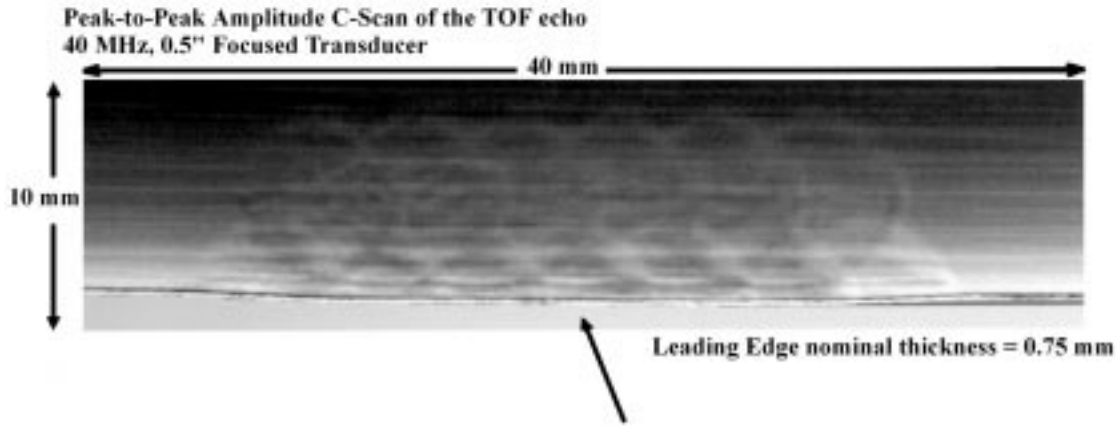

Fig. 19 NDI C-scan for the 9 GW/cm^2-5 shock/spot treatment from the current study

Since LSP relies on the constraint from surrounding material, component distortion due to LSP will necessarily increase with treatment intensity and the size of the treated area since the LSP-treated volume will be constrained by a continually reduced volume. If large areas are subjected to LSP, it may become necessary to account for this distortion in the initial component design.

With regard to the present study, with the exception of the 9 GW/cm^2-5 shock condition, none of the LSP treatments produced readily apparent distortion greater than mild imprints coincident with the location of the laser pulses. With the more mild treatments, not even these were readily apparent. In the case of the 9 GW/cm^2-5 shock condition, the LSP treatment induced a slight extrusion of the leading edge in the treated region, as can be seen in Fig. 19.

4.2 Microstructure

Although no change in phase content or morphology was detected at the SEM level, in previous LSP work in titanium alloys with a higher vanadium content (on the order of 12 wt.%), a fine dispersion of metastable ω phase has been identified.[15] It is not believed that the ω phase is present in the current alloy due to the relatively low vanadium content, but this remains to be verified through further studies using transmission electron microscopy.

4.3 Residual Stresses

Residual-stress distributions were found to be a strong function of both laser intensity and pulse repetition. The 9 GW/cm^2-3 and 5 shock trials generated the most intense compressive residual stresses of the treatments studied, while the 4 GW/cm^2-1 shock trial generated the least intense.

For the LSP conditions studied, the effect of laser intensity on the maximum magnitude of the compressive residual stress was found to be greater than that of shock repetition. By way of example, except for the persistence of the compressive residual stress at depth, the 9 GW/cm^2-1 shock treatment was largely identical to the 4 GW/cm^2-3 and 5 shock treatments.

Much as in the case of traditional shot peening, repeated laser shocks would be expected to increase the magnitude of the surface and subsurface compressive residual stresses until a treatment intensity-dependent saturation point is reached. This hypothesis proved to be correct. While there was a significant residual-stress benefit in moving from 1 to 3 shocks/spot, both in terms of the magnitude of the surface residual stresses and the magnitude of the compressive stresses at depth, the 5 shocks/spot treatments offered little or no improvement over the 3 shock condition, yet induced some additional cold work and distortion.

Both the 4 and 9 GW/cm^2-1 shock treatments failed to place the entire through-thickness of the leading edge into residual compression. Additionally, both 1 shock/spot treatments produced essentially identical residual-stress profiles at depths greater than 0.1 mm from the surface. Based on this, one could conclude that increasing laser intensity alone is insufficient to produce through-thickness compressive residual stresses and that repeated shocking is necessary to accomplish this.

Through-thickness compressive residual stresses (in the x direction, as indicated in Fig. 3) are desirable, particularly for the geometry studied here. This is because, for residual-stress states where the entire thickness is not in compression, there may be fatigue initiation sites available at FOD sites that are at a zero or even tensile state of residual stress. This is not only expected to reduce the potential effectiveness of the laser peening at resisting subsequent fatigue damage, but, additionally, fatigue cracks might "tunnel" underneath the zone of compression. This could result in a condition that could be quite dangerous in service, wherein fatigue cracks might be present but may not be detectable by a visual or tactile surface inspection.

With respect to the saturation of the compressive residual stresses when pulse repetition is increased from 3 to 5, one can speculate as to the possible mechanisms involved. It is likely the saturation effect is a result of strain hardening. The first shock wave that travels through the thickness of the specimen will cause the greatest amount of plasticity (strain hardening) in the near surface of the specimen. The energy dissipated by this plasticity will rapidly reduce the magnitude of the shock wave to the point where, in the midthickness regions, only elastic deformation will occur. Upon the application of a second laser pulse, the shock wave again travels through the near

surface layer, only this time there are fewer available mechanisms for plasticity in the strain-hardened near-surface layers, and as a result, more plasticity is induced internally. Once all the plasticity mechanisms that are active at a given peak stress are exhausted, repeated shocking will cause elastic deformation almost exclusively. From the residual-stress data generated by this program, it appears that, for the conditions studied, saturation typically occurs at 3 shocks/spot. The peak levels of plasticity induced in the surface layers are expected to be greater than those induced in the midthickness due to the relative lack of constraint and the fact that the surface is subjected to the highest shock pressures, barring shock-wave superposition effects.

4.4 Cold Work

With respect to cold work, previous work by Prevéy *et al.*[2] on several aerospace alloys, including Ti-6Al-4V, found that the thermal stability of compressive residual stresses induced by mechanical surface treatments was inversely proportional to the level of cold work. In effect, as the cold work level decreased, the thermal stability of the compressive stress state increased. Indeed, for Ti-6Al-4V, LSP treatments inducing less than 5% cold work were found to offer excellent thermal stability, particularly when compared to surface treatments that induce extremely high levels of surface cold work (*e.g.*, shot peening). Applying this criterion to the current study, it is expected that the 4 GW/cm^2 LSP conditions should produce compressive stresses with acceptable levels of thermal stability. The 9 GW/cm^2 treatments, by inducing levels of cold work in the 10 to 20% range, become less attractive for higher temperature applications due to anticipated loss of thermal stability. However, the previously mentioned study[2] indicated that for reasonably high service temperatures (325 °C in the case of Ti-6Al-4V), surface treatment methods inducing these levels of cold work may produce compressive stresses with adequate levels of thermal stability.

The increase in cold work with increasing laser intensity and pulse repetition is expected since the intensity of the pressure pulse associated with the vaporization of the opaque layer has been shown to increase by the square root of the laser-beam power density (until the onset of dielectric breakdown of the transparent constraining layer).[12] As such, a more intense shock wave could be expected to cause greater plastic strain than a weaker one. Further, since cold work is cumulative, repeated shocking could be expected to induce additional cold work in the material.

5. Summary and Conclusions

Ti-6Al-4V simulated airfoils were laser shock peened with an Nd:phosphate glass laser (λ = 1.054 μm) at two intensities (4 and 9 GW/cm^2) and 3 pulse repetition treatments (1, 3, and 5 shocks/spot) per intensity. While the most intense treatments did result in some modest levels of distortion of the airfoil, no cracking or internal delaminations were detected in any of the specimens. Additionally, the microstructure remained essentially unchanged.

It was found that the residual-stress state and percent cold work, with the exception of the 5 shock/spot treatments, increased with both the LSP power density and the number of laser pulses/spot. The 5 shock/spot treatments were very similar in terms of in-depth residual stresses and cold work to the 3 shock/spot treatments at the same laser intensity. In addition, there was a strong correlation between the magnitude of residual compressive stresses generated and the percent cold work measured.

The most intense states of compressive residual stress were produced by the 9 GW/cm^2-3 and 5 shocks/spot LSP conditions. Both of these treatments generated higher cold work than any of the 4 GW/cm^2 conditions. For both the 4 and 9 GW/cm^2 laser intensities, there were no benefits, residual stress or otherwise, to the 5 shock/spot treatments.

The least intense state of compressive residual stress was found for the 4 GW/cm^2-1 shock condition. This treatment (along with the 9 GW/cm^2-1 shock condition) did not produce a residual state of compression throughout the entire thickness of the simulated airfoil specimen. However, this least intense LSP condition did result in the lowest distortion and cold work in the study.

References

1. A. Turnbull, E.R. de los Rios, R.B. Tait, C. Laurant, and J.S. Boabaid: *Fatigue Fract. Eng. Mater. Structures*, 1998, vol. 21, pp. 1513-24.
2. P.S. Prevéy, D. Hornbach, and P. Mason: *Thermal Residual Stress Relaxation and Distortion in Surface Enhanced Gas Turbine Components*, ASM/TMS Materials Week, Indianapolis, IN, 1997.
3. H. Hanagarth, O. Vöringer, and E. Macherauch: in *Shot Peening*, K. Iida, ed., The Japanese Society of Precision Engineering, Tokyo, 1993, pp. 337-45.
4. A.H. Clauer, J.K. Lee, R.A. Brockman, W.R. Braisted, S.A. Noll, and A. Gilat: *Proc. 5th Nat. Turbine Engine High Cycle Fatigue (HCF) Conf.*, Chandler, AZ, Mar. 2000.
5. A.H. Clauer, J.H. Holbrook, and B.P. Fairand: in *Shock Waves and High-Strain-Rate Phenomena in Metals*, M.A. Meyers and L.E. Murr, eds., Plenum Publishing Corp., New York, NY, 1981, pp. 675-702.
6. P. Peyre and R. Fabbro: *Optical and Quantum Electronics*, 1995, vol. 27, pp. 1213-29.
7. D. Eylon: "Summary of the Available Information on the Processing of the Ti-6Al-4V HCF/LCF Program Plates," University of Dayton, Dayton, OH.
8. J.R. Ruschau, R. John, S. Thompson, and T. Nicholas: *J. Mater. Technol.*, 1999, vol. 121, pp. 321-29.
9. P.R. Smith, M.J. Shepard, P.S. Prevéy, and A.H. Clauer: *J. Mater. Eng. Performance*, 2000, vol. 9 (1), pp. 33-37.
10. John Ruschau: University of Dayton Research Institute, Dayton, OH, personal communication, 2000.
11. A.H. Clauer: in *Surface Performance of Titanium*, J.K. Gregory, H.J. Rack, and D. Eylon, eds., TMS, Warrendale, PA 1996, pp. 217-30.
12. B.P. Fairand and A.H. Clauer: *J. Appl. Phys.*, 1979, vol. 50 (3), pp. 1497-1502.
13. P.S. Prevéy: *Metals Handbook*, ASM, Metals Park, OH, 1986, vol. 10, pp. 380-92.
14. P. Prevéy: *Residual Stress in Design, Process & Material Selection*, ASM, Metals Park, OH, 1987, pp. 11-19.
15. A.H. Clauer and B.P. Fairand: "Pulsed Laser Interactions With Titanium-Vanadium Alloys," Final Report for U.S. Army Research Office Grant Nos. DAAG29-77-G-0187 and DAHC04-75-G-0115, Feb. 15, 1975, U.S. Army Research Office, Research Triangle Park, NC.